JOC The Journal of Organic Chemistry

ARTICLE

pubs.acs.org/joc

Orbital Interactions in Selenomethyl-Substituted Pyridinium Ions and Carbenium Ions with Higher Electron Demand

S. Fern Lim, Benjamin L. Harris, Paul Blanc, and Jonathan M. White*

School of Chemistry and Bio-21 Institute, University of Melbourne, Parkville 3010 Melbourne, Australia

Supporting Information

ABSTRACT: Computational, solution phase, and crystal structure analysis of 2- and 4-organoselenylmethyl-substituted pyridinium ions (**10a**−**c** and **11a**−**c**) provides strong evidence for C−Se hyperconjugation ($\sigma_{C-Se}-\pi^*$) between the C−Se σ-bond and the π-deficient aromatic ring and a through-space interaction ($n_{Se}-\pi^*$) between the selenium p-type lone pair and the π-deficient aromatic ring. There is also a weak anomeric-type interaction ($n_{Se}-\sigma^*_{CC}$) involving the selenium p-type lone pair electrons and the polarized $CH_2-C(Ar)$ σ-bond. NBO analysis of calculated cations with varying electron demand (B3LYP/6-311++G**) show that C−Se hyperconjugation ($\sigma_{C-Se}-\pi^*$) is the predominant mode of stabilization in the weakly electron-demanding pyridinium ions (**10d**, **11d**, **14**, and **15**); however, the through-space ($n_{Se}-\pi^*$) interaction becomes more important as the electron demand of the β-Se-substituted carbocation increases. The anomeric interaction ($n_{Se}-\sigma^*_{CC}$) is relatively weak in all ions.

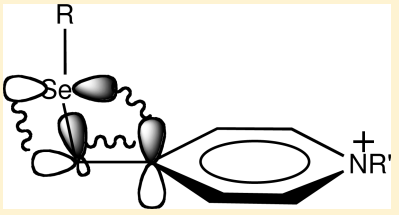

INTRODUCTION

We have reported previously that unimolecular solvolysis of the conformationally biased and nonbiased β-phenylselenyl trifluoroacetates **1** and **2** occurs at rates which are 10^7 and 10^6 respectively with respect to the unsubstituted derivative **3** indicating that the selenium substituent strongly assists in the departure of the leaving group.[1]

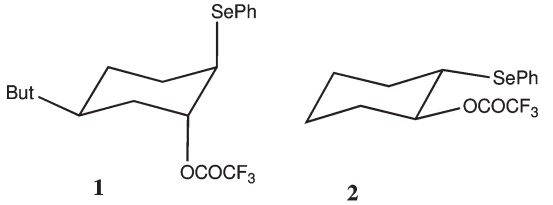

Conventionally, participation by the selenium substituent in these solvolyses occurs by the bridged ion intermediate **4** (Scheme 1), in which the selenium lone pair electrons facilitate the departure of the leaving group. This is an example of nonvertical neighboring nucleophilic participation.[2] However, we considered the possibility that participation by the selenium substituent might occur by σ_{C-Se}−p hyperconjugation (vertical participation)[3] and involve the open carbenium ion intermediate **5**, so that the neighboring nucleophile may be the loosely held electrons of the C−Se σ-bond rather that the selenium lone pair. This mode of stabilization of the intermediate carbenium ion **5** is analogous to that provided by the trimethylsilyl substituent in the ion **7**, which is the basis of the silicon β-effect.[4] Woerpel and co-workers have raised similar questions regarding the nature of sulfur participation in *S*-glycoside chemistry.[5]

Strong evidence that the C−Se bond is a good σ-donor orbital, and therefore capable of effectively stabilizing positive charge by hyperconjugation, was provided by crystallographic analysis of a range of ester and ether derivatives of the alcohol **6**[1] using the variable oxygen probe.[6] However, whether the solvolysis of **1** involves the bridged cation **4** the open cation **5** is still an open question.

We have found that substituted *N*-methyl pyridinium ions **8** provide a convenient system for investigating the effects of C−M (M = Si, Ge) hyperconjugation.[7] For example, conversion of the trialkylsilyl-substituted pyridine derivatives **9** into the ion **8a** results in a significant downfield shift in the ^{29}Si NMR spectrum, and a significant decrease in the ^{29}Si−^{13}C one-bond coupling constant between the silicon and the methylene carbon. These spectroscopic effects are consistent with significant contribution of the double-bond−no-bond resonance form **8a′** to the structure of these ions. Furthermore, X-ray structure analysis of these ions reveals that the R_3Si-CH_2Pyr bond distance in ions **8a** is significantly lengthened relative to standard values.

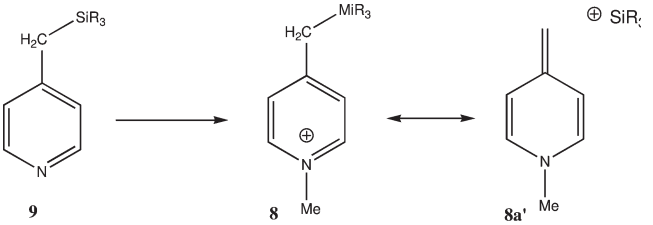

Received: November 26, 2010
Published: February 11, 2011

Scheme 1. Possible Modes of Neighboring Group Participation by the β-Phenylselenyl Substituent

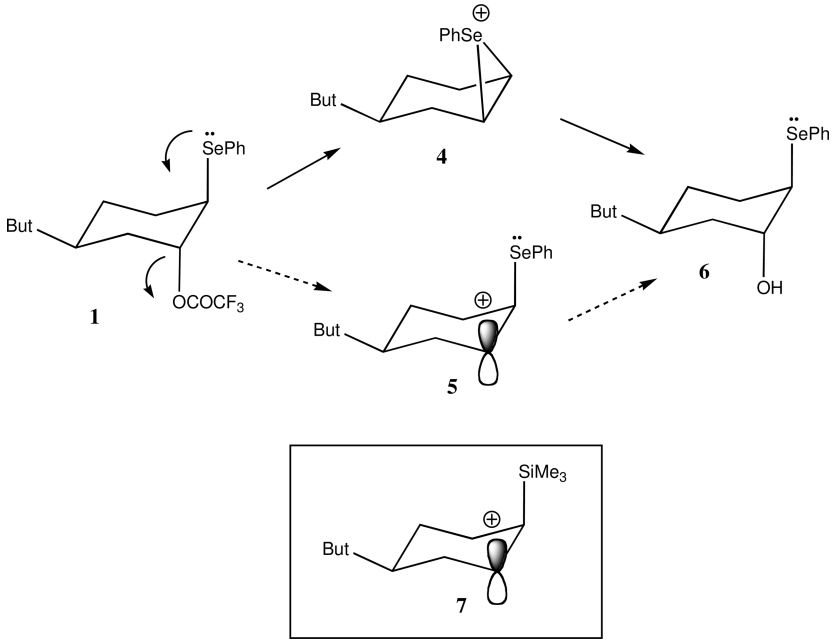

Scheme 2. Syntheses of Selenylmethyl-Substituted Pyridines 12a−c and 13a−c and Pyridinium Ions 10a−c and 11a−c[a]

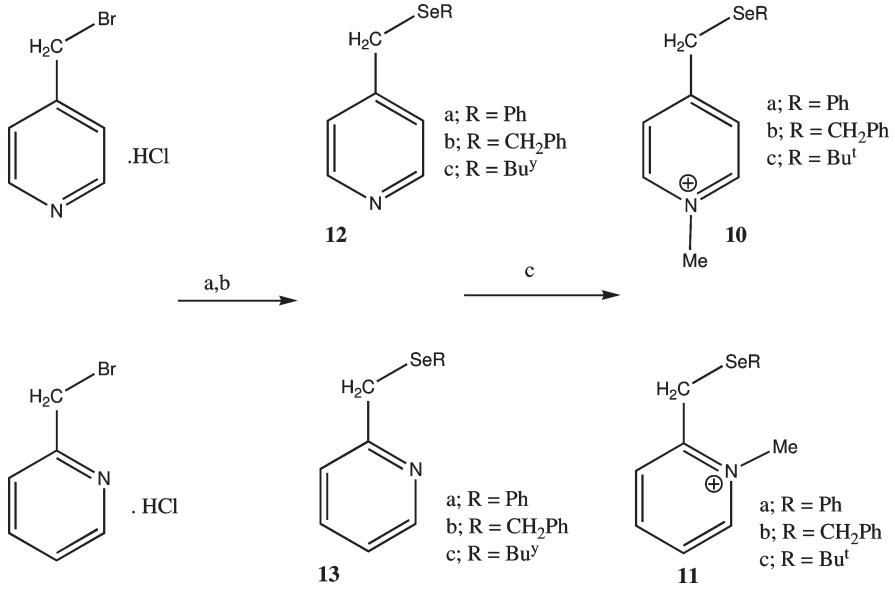

[a] Reagents and conditions: (a) NaOH, MeOH; (b) RSeNa; (c) CH_3I, or $CH_3OSO_2CF_3$, or CH_3OTs.

Thus to provide further evidence for stabilization by $\sigma_{C-Se}-p$ hyperconjugation we proposed to carry out an experimental and computational study on the 2- and 4-alkyl- and aryl-selenylmethyl-substituted pyridinium ions **10a−c** and **11a−c**.

RESULTS AND DISCUSSION

The precursor pyridine derivatives **12a−c** and **13a−c** were prepared according to Scheme 2; these were then converted into **10a−c** and **11a−c** respectively by methylation using either methyl iodide, methyl tosylate, or methyl triflate for both solution phase and crystallographic analysis.

The ^{77}Se chemical shifts, and $^{77}Se-^{13}C$ one-bond coupling constants for **10a−c** and **11a−c** and the pyridine precursors **12a−c** and **13a−c** are presented in Table 1.

The ^{77}Se chemical shifts for the 4-selenomethyl-substituted *N*-methyl pyridinium ions **10a−c** are deshielded relative to their neutral precursors **12a−c** by 45.6, 38.8, and 36.4, respectively, consistent with dispersal of the positive charge on the pyridinium ring onto the selenium substituent. Interestingly, however, while methylation of the 2-phenylselenomethylpyridine derivative **13a** also results in a downfield shift of the ^{77}Se chemical shift in the resulting ion **11a**, the remaining two

dx.doi.org/10.1021/jo102307v |J. Org. Chem. 2011, 76, 1673–1682

derivatives **11b,c** display an upfield shift upon methylation of the precursors **13b,c**. This upfield shift possibly arises due to steric interaction of the ortho *N*-methyl substituent with the selenomethyl substituent in **13b−c**, an example of a ^{77}Se γ gauche effect,[8] which has been demonstrated in other systems. If the pyridine derivatives are converted to their corresponding pyridinium ions by protonation rather than methylation, then the steric environment surrounding the 4-substituted derivatives and the 2-substituted derivatives becomes essentially identical. Consistent with this, protonation of 4-substituted pyridines **12b,c** and 2-substituted pyridine derivatives **13b,c** results in a downfield shift of the ^{77}Se by ca. 40 ppm magnitudes for all ions (see the Experimental Section).

The downfield shift of the ^{77}Se signal upon conversion of the pyridine precursors **12a−c** and **13a−c** to their corresponding positively charges pyridinium ion derivatives is consistent with the dispersal of positive charge onto the selenium substituent. However, associated with this downfield shift is a small increase in the one-bond ^{77}Se−^{13}C one-bond coupling constant, in direct contrast to the effects observed in the silicon-substituted ion **8a** where there is a significant decrease in the ^{29}Si−^{13}C one-bond coupling constant compared with its neutral precursor **9a**. This result appears to conflict with the expectations of $\sigma_{C-Se}-\pi$ hyperconjugation in these ions, such that contributions of the proposed double-bond−no-bond resonance forms **10′** and **11′** to the ground state structures of the ions **10** and **11** (Figure 1) should weaken the Se−CH_2 bond and hence decrease the ^{77}Se−^{13}C coupling constant. It is likely that ^{13}C−^{77}Se coupling constants are influenced by factors other than hyperconjugation, which may also change upon conversion of the neutral pyridines into the pyridinium ions, for example the hybridization state of the lone pairs on the selenium is known to effect both the fermi-contact term and the spin dipole term of the ^{77}Se−^{13}C coupling constant;[9] these effects may mask the effects of hyperconjugation, and some insight to this is provided in the structural and computational studies described below.

Table 1. δ ^{77}Se NMR Chemical Shifts and ^1J CH_2−Se Coupling Constants for the Selenylmethyl-Substituted Pyridines 12a−c and 13a−c and the Pyridinium Ions 10a−c and 11a−c

CMPD	^1J C−Se	δ ^{77}Se	CMPD	^1J C−Se	δ ^{77}Se	ΔJ (Hz)	$\Delta\delta$ ^{77}Se
12a	61.9	361.2	**10a**	65.5	406.8	+3.6	+45.6
12b	65.5	338.1	**10b**	67.0	376.9	+1.5	+38.8
12c	67.3	458.6	**10c**	70.9	495.0	+2.6	+36.4
13a	61.9	337.2	**11a**	67.7	364.9	+5.8	+27.9
13b	64.8	331.3	**11b**	60.3	312.2	−4.5	−19.1
13c	67.7	448.1	**11c**	70.5	443.3	+2.8	−4.8

To gain further insight into the nature of the interaction between the selenium substituent and the electron-deficient pyridinium ring we determined the X-ray crystal structures of the ions **10** and **11**. Crystals of suitable quality for X-ray analysis were obtained for the *N*-methyl pyridinium ions **10b−c**, **11a**, and **11c**; in addition to these we obtained crystals for the corresponding protonated pyridinium ions **12aH** and **13aH** and **13bH** as their picrate salts. Thermal ellipsoid plots for all structures are presented in Figure 2 while selected bond distances, bond angles, and dihedral angles are presented in Table 2.

In all the structures the Se−CH_2 bond is close to orthogonal to the pyridinium ring, a conformation that allows for effective overlap between the Se−CH_2 σ-bond and the low-lying π^* -system (Figure 3). The mean Se−CH_2 bond distance is 1.973 Å while the mean CH_2−C_{ipso} distance is 1.485 Å; comparison of these values for a typical Se−CH_2 distance (1.960 Å) and CH_2−Ar distance (1.500 Å), which were obtained from the Cambridge Crystallographic Database,[10] provides some evidence for contributions of the double-bond−no-bond resonance structures **10′** and **11′** to the ground state structures of these ions. Of interest was the unusual conformation about the Se−CH_2 bond, which adopted the sterically less-favored gauche arrangement in five of the seven structures, the exceptions being **10c** and **11c** where R = Bu^t. The preference for the gauche conformation in **11a** may have its origins in intramolecular $\pi-\pi$ interactions; however, this is not the case for the remainder of the structures. We considered that this conformation may be favored for one or both of the following reasons (Figure 3): (i) it allows for the p-type lone pair on the selenium to interact with the CH_2−Ar antibonding orbital (analogous to the anomeric effect)[11] and/or (ii) it allows for a through-space interaction between the selenium p-type lone-pair and the low-lying π-system of the positively charged pyridinium ring—a similar type of through space orbital interaction ($n_{Se}-\pi^*_{CO}$) has been used to explain the conformational preferences of α-phenylselenylcyclohexanones.[12,13] It is compelling to propose the presence of the $n_{Se}-\sigma^*_{CC}$ as this may help to explain the unexpected effects on the Se−CH_2 coupling constants (Table 1) which increased upon methylation of the pyridine precursors (**12a−c** and **13a−c**), this interaction that would strengthen the Se−CH_2 bond may offset the expected bond weakening effects of $\sigma_{C-Se}-\pi^*$ hyperconjugation.

COMPUTATIONAL DETAILS

To gain further insight into the structures of these ions, and the importance of the various orbital interactions between the selenium substituent and the electron deficient pyridinium ring, we carried out ab initio molecular orbital calculations on the model systems **10d** and **11d**

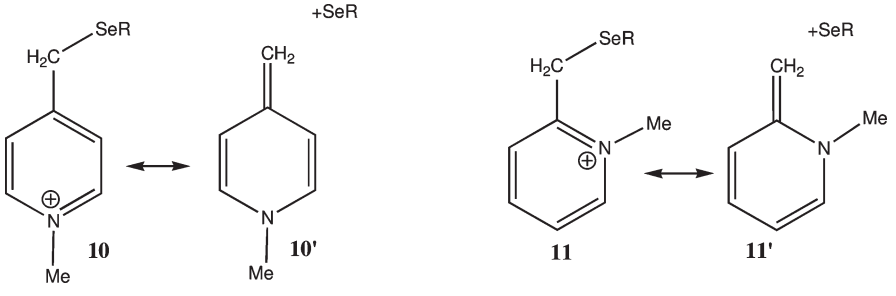

Figure 1. Hyperconjugation in 2- and 4-selenomethylpyridinium ions.

dx.doi.org/10.1021/jo102307v |*J. Org. Chem.* 2011, 76, 1673–1682

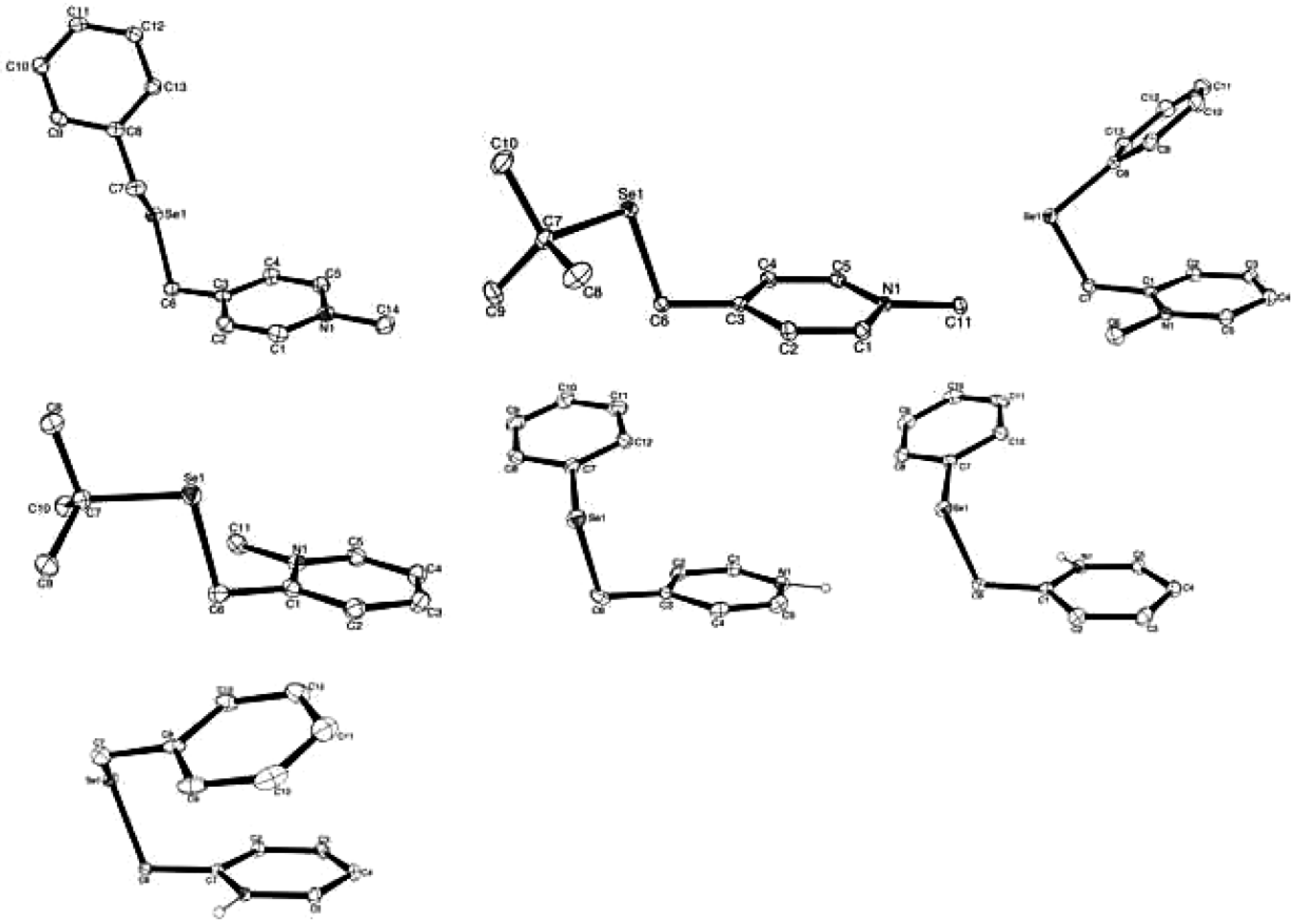

Figure 2. Thermal ellipsoid plots for **10b**, **10c**, **11a**, **11c**, **12aH**, **13aH**, and **13bH**. Ellipsoids are at the 20% probability level; counterions have been omitted for clarity.

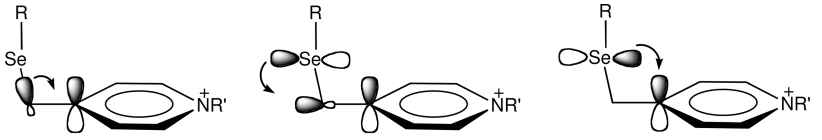

Figure 3. Possible orbital interactions involving the selenium substituent in the pyridinium ions **10a**−**c** and **11a**−**c** (R′ = Me) and **12aH**, **13aH**, and **13bH** (R′ = H).

Table 2. Selected Distances (Å), Angles (deg), and Dihedral Angles (deg) for the Selenium-Substituted Pyridinium Ions[a]

	10b	10c	11a	11c	12aH	13aH	13bH
Se−CH_2	1.959(3)	1.967(3)	1.977(2)	1.971(3)	1.989(6)	1.982(2)	1.969(2)
CH_2−C_{ipso}	1.483(3)	1.483(4)	1.479(2)	1.495(4)	1.486(8)	1.483(3)	1.489(2)
Se−CH_2−C_{ipso}	112.7(3)	109.7(2)	110.5(1)	107.1(2)	110.3(4)	111.5(1)	112.0(2)
Se−CH_2−C_{ipso}−C_{ortho}	−61.3(3)	93.0(2)	−102.3(2)	98.0(2)	−100.0(4)	84.7(1)	73.5(2)
R−Se−CH_2−C_{ipso}	−67.2(3)	−141.2(2)	44.9(1)	154.1(2)	76.3(4)	93.0(1)	−77.6(2)

[a] Estimated standard deviations are in parentheses.

(R = Me); in addition to these we also carried out the calculations on structures **14**−**18** in order to assess the effects that increasing the electron demand of the cations has on the magnitude of these interactions.

Calculations were performed at the B3LYP/6-311++G** level of theory,[14] a level of theory that has been previously employed to investigate stereoelectronic effects of chalcogen substituents;[15] energies

are ZPE corrected. Natural Bond Orbitals (NBOs) were calculated by using the NBO 3.0 program[16] as implemented in the GAUSSIAN 03 package.[17] Calculated structures for **10d** and **18** are presented in Figure 4. The remaining structures **11d** and the cations **14**−**18** with relevant structural parameters are available in the Supporting Information; both the anti and gauche conformations about the Se−CH_2 bond were calculated. In all cases the gauche conformation was found to be more stable than the anti conformation with the energy difference between the two conformations increasing with increasing electron demand of the carbenium ion.

For the pyridinium ion **10d**, which has low electron demand, the anti conformation is a local minimun that lies ca. 0.7 kJ/mol above the gauche conformation, and a rotation barrier of 4 kJ/mol separates these two conformations; interestingly in the cyclopropenyl cation **18** the anti conformation is an energy maxima that is 12.4 kJ above the two degenerate gauche conformations (see the Supporting Information for energy barriers). Selected structural parameters and NBO interaction energies for the $\sigma_{Se-C}-\pi^*$, $n_{Se}-\sigma^*_{CC}$, and $n_{Se}-\pi^*$ orbital interactions (as shown in Figure 3) for the calculated structures for **10d**, **11d**, and **14**−**18** are presented in Table 3.

Examination of the NBO interaction energies in Table 3 shows that the most important interaction in the methylselenylmethyl-substituted pyridines **10d** and **11d** is $\sigma_{Se-C}-\pi^*$ hyperconjugation, with the through-space $n_{Se}-\pi^*$ and the $n_{Se}-\sigma^*_{C-C}$ interactions being relatively weak. The presence of the $n_{Se}-\pi^*$ and $n_{Se}-\sigma^*_{CC}$ interactions, although weak, however explains the preference of the pyridinium ions **10b**, **11a**, **12aH**, **13aH**, and **13bH** to adopt the gauche conformation in the solid state, and the observation that **10c** and **11c** with the sterically more demanding tBu-Se substituents prefer to adopt the antiperiplanar conformation. As the electron demand of the cations increases (as gauged by the decreasing pK_{R^+} values for the parent cations), both the hyperconjugative $\sigma_{Se-C}-\pi^*$ and through-space $n_{Se}-\pi^*$ orbital interactions increase in strength while the $n_{Se}-\sigma^*_{C-C}$ interaction remains small throughout the series. Increasing C−Se−π hyperconjugation with increasing electron demand is clearly demonstrated in Figure 5, where the Se−CH_2 bond distance increases with decreasing pK_{R^+}.

The increasing through-space ($\sigma_{Se-C}-\pi^*$) interaction with electron demand of the cation manifests as a closing up of the Se−CH_2−C(+) bond angle, which is clearly shown by the plot of the Se−CH_2−C(+) bond angle vs pK_{R^+} (Figure 6). This appears to represent the early stages of bridging by the β-selenium substituent.

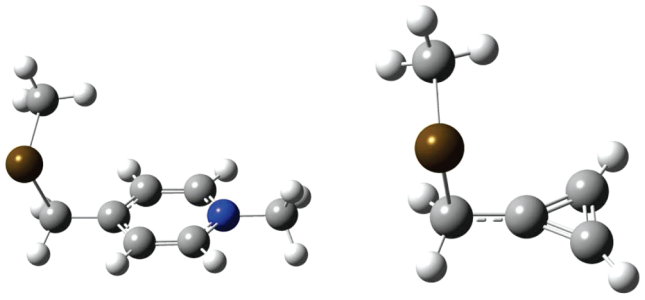

Figure 4. Calculated structures (B3LYP/6-311++G**) for cations **10d** and **18**.

CONCLUSION

Lengthening of the Se−CH_2 bond and shortening of the CH_2−C(Ar) bond in the solid state structures of selenomethyl-substituted pyridinium ions provides evidence for carbon−selenium hyperconjugation ($\sigma_{C-Se}-\pi^*$) between the carbon−selenium bonding orbital and the π^* orbital of the electron-deficient pyridinium ring. In addition there are interactions involving the selenium p-type nonbonded pair of electrons including a through-space $n_{Se}-\pi^*$ interaction with the electron-deficient pyridinium ring and an anomeric interaction ($n_{Se}-\sigma^*_{CC}$) with the vicinal CH_2−C(Ar) antibonding orbital. We believe that these latter interactions are responsible for the selenium substituent adopting the gauche conformation in **10a,b** and **11a,b**, but are weak enough that the *tert*-butyl-substituted derivatives (**10c** and **11c**) adopt the sterically more preferred anti conformation. In solution a significant downfield shift in the ^{77}Se NMR chemical shift upon conversion of the pyridine precursors into the positively pyridinium ions is consistent with dispersal of positive charge on the selenium nucleus, consistent with all the orbital interactions discussed above. Calculations show that C−Se hyperconjugation ($\sigma_{C-Se}-\pi^*$) is the predominant mode of stabilization in the pyridinium ions (**10d**, **11d**, **14**, and **15**); however, the through-space ($n_{Se}-\pi^*$) interaction becomes more

Table 3. Selected Distances (Å), Angles (deg), and Dihedral Angles (deg) for the Calculated Structures of 10d, 11d, and 14−18[a]

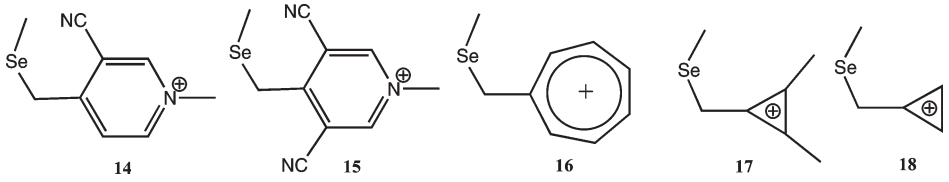

14 15 16 17 18

	10d	11d	14	15	16	17	18
pK_{R^+}	20.5[18]	18[b]	12.2[19]	3.5[19]	4.7[20]	7.8[21]	−7.4[22]
Se−CH_2	1.9995	2.0038	2.0048	2.0091	2.0088	2.0074	2.0145
CH_2−C+	1.4871	1.4889	1.4818	1.4783	1.4829	1.4572	1.4462
Se−CH_2−C^+	109.92	112.32	107.90	106.34	103.60	104.47	101.13
Se−CH_2−C^+−C	100.17	−99.72	96.56	93.4	91.6	93.4	91.2
CH_3−Se−CH_2−C^+	74.78	71.25	79.95	85.77	99.3	85.77	88.13
$\sigma_{Se-C}-\pi^*$	34.8	34.2	43.4	43.4	55.3	70.9	104.9
$n_{Se}-\pi^*$	9.0	8.8	14.8	14.8	37.1	48.5	73.7
$n_{Se}-\sigma^*_{C-C}$	12.6	14.8	11.9	10.6	11.8	10.1	6.0

[a] NBO stabilization energies for the $\sigma_{Se-C}-\pi^*$, $n_{Se}-\sigma^*_{CC}$, and $n_{Se}-\pi^*$ orbital interactions are given in kJ mol^{-1}. Structures were calculated at B3LYP/6-311++G** for all atoms except for Se, which was calculated with the SDD basis set. [b] An approximated value.[19]

dx.doi.org/10.1021/jo102307v |J. Org. Chem. 2011, 76, 1673–1682

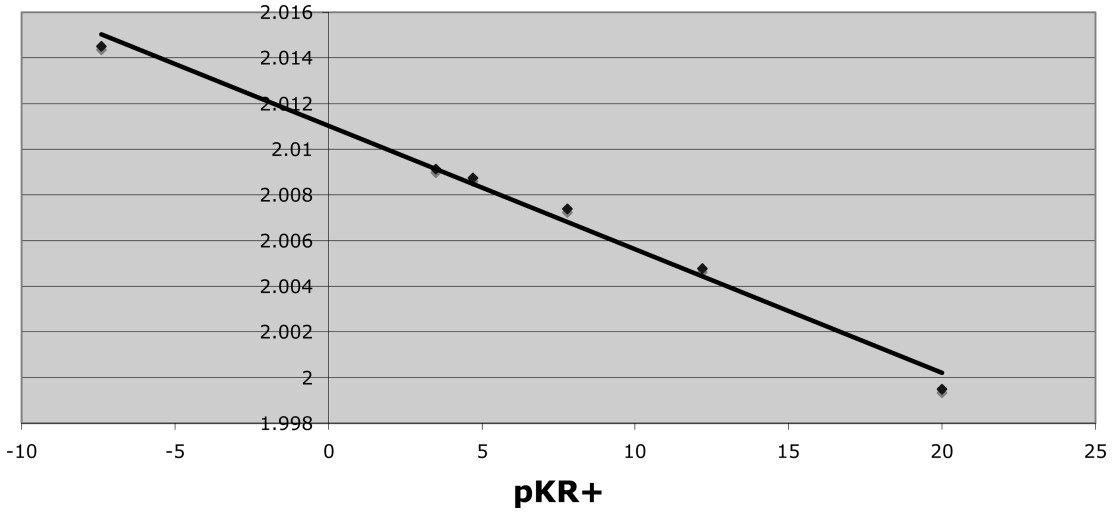

Figure 5. Plot of Se−CH_2 bond distance (Å) vs pK_{R^+} for the parent cation for the cations **10a** and **14**−**18**.

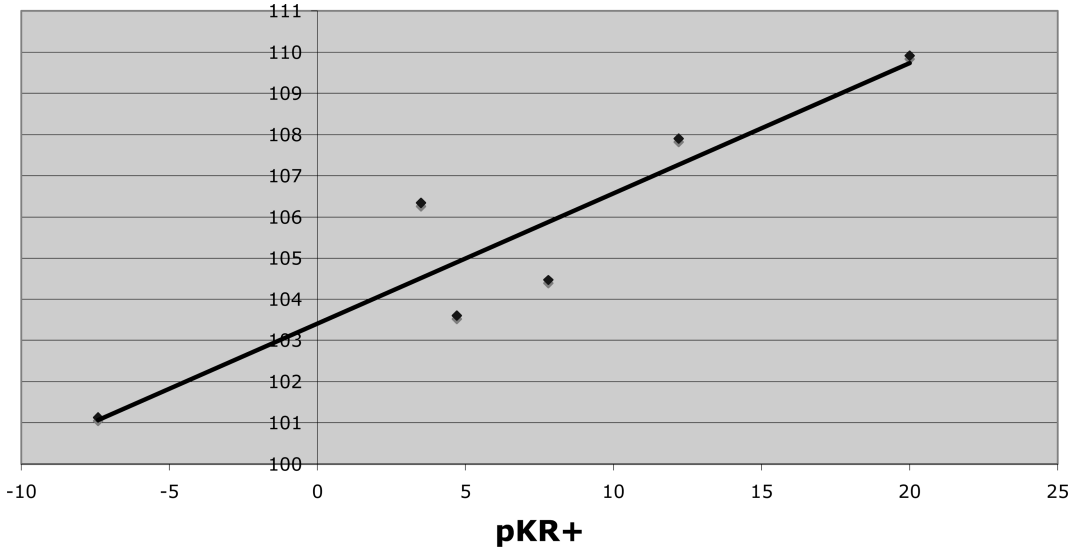

Figure 6. Plot of Se−CH_2−C(+) bond angle (deg) vs pK_{R^+} for the parent cation, for the cations **10a** and **14**−**18**.

important as the electron demand of the β-Se-substituted carbocation increases. The anomeric interaction ($n_{Se}-\sigma^*_{CC}$) is relatively weak in all ions.

EXPERIMENTAL SECTION

a. Crystallography. Intensity data were collected with an Oxford Diffraction Sapphire CCD diffractometer, using Cu Kα radiation (graphite crystal monochromator λ = 1.54184 Å), or with a Bruker SMART Apex CCD detector, using Mo Kα radiation (graphite crystal monochromator λ = 0.71073 Å). The temperature during data collection was maintained at 130.0(1) K for all data collections by using an Oxford Cryostream low-temperature device.

Crystal data for **10b** (triflate): $C_{15}H_{16}F_3NO_3SSe$, M = 426.31, T = 130.0(2) K, λ = 1.5418 Å, monoclinic, space group $P2_1/c$, a = 14.8030(5) Å, b = 8.9842(3) Å, c = 13.0040(4) Å, β = 99.476(3)°, V = 1705.84(10) Å^3, Z = 4, D_c = 1.660 Mg M^{-3}, μ(Cu Kα) = 4.551 mm^{-1}, F(000) = 856, crystal size 0.69 × 0.25 × 04 mm^3; 9296 reflections measured, 3284 independent reflections (R_{int} = 0.0465), the final R was 0.0436 [$I > 2\sigma(I)$] and $wR(F^2)$ was 0.1244 (all data).

Crystal data for **10c** (tosylate): $C_{18}H_{25}NO_3SSe$, M = 414.41, T = 130.0(2) K, λ = 0.71073 Å, monoclinic, space group $P2_1/n$, a = 6.509(2) Å, b = 33.521(8) Å, c = 8.747(2) Å, β = 93.464(4)°, V = 1905.0(8) Å^3, Z = 4, D_c = 1.445 Mg M^{-3}, μ(Cu Kα) = 2.096 mm^{-1}, F(000) = 856, crystal size 0.5 × 0.4 × 0.03 mm^3; 11914 reflections measured, 4354 independent reflections (R_{int} = 0.0372), the final R was 0.0407 [$I > 2\sigma(I)$] and $wR(F^2)$ was 0.1023 (all data).

Crystal data for **11a** (triflate): $C_{14}H_{14}F_3NO_3SSe$, M = 412.28, T = 130.0(2) K, λ = 0.71073 Å, monoclinic, space group $P2_1/c$, a = 10.369(3) Å, b = 11.734(3) Å, c = 13.532(4) Å, β = 105.156(4)°, V = 1589.2(7) Å^3, Z = 4, D_c = 1.723 Mg M^{-3}, μ(Mo Kα) = 2.538 mm^{-1}, F(000) = 824, crystal size 0.40 × 0.40 × 0.30 mm^3; 8157 reflections measured, 2798 independent reflections (R_{int} = 0.0213), the final R was 0.0238 [$I > 2\sigma(I)$] and $wR(F^2)$ was 0.0686 (all data).

Crystal data for **11c** (tosylate): $C_{18}H_{25}NO_3SSe$, M=414.41, T=130.0(2) K, λ = 1.5418 Å, monoclinic, space group $P2_1/c$, a = 17.4160(3) Å, b = 9.5355(2) Å, c = 11.4018(2) Å, β = 90.467(2)°, V = 1893.44(6) Å^3, Z = 4, D_c = 1.454 Mg M^{-3}, μ(Cu Kα) = 3.843 mm^{-1}, F(000) = 856, crystal size 0.41 × 0.25 × 03 mm^3; 8219 reflections measured, 3690 independent reflections (R_{int} = 0.0358), the final R was 0.0400 [$I > 2\sigma(I)$] and $wR(F^2)$ was 0.0964 (all data).

Crystal data for **12aH** (picrate): $C_{18}H_{14}N_4O_7Se$, M = 477.29, T = 130.0(2) K, λ = 0.71073 Å, monoclinic, space group $P2_1/n$, a = 7.449(3) Å, b =13.527(4) Å, c = 19.221(6) Å, β = 99.285(5)°, V = 1911(1) Å^3, Z = 4, D_c = 1.659 Mg M^{-3}, μ(Mo Kα) = 2.016 mm^{-1}, F(000) = 960, crystal size 0.40 × 0.25 × 0.05 mm^3; 9186 reflections measured, 3353 independent reflections (R_{int} = 0.1140), the final R was 0.0585 [$I > 2\sigma(I)$] and $wR(F^2)$ was 0.1190 (all data).

Crystal data for **12bH** (picrate): $C_{18}H_{14}N_4O_7Se$, M = 477.29, T = 130.0(2) K, λ = 0.71073 Å, triclinic, space group $P\bar{1}$, a = 8.2176(5) Å, b = 9.7350(6) Å, c =12.3328(8), Å, α = 82.277(1)°, β = 83.488(1)°, γ = 72.756(1)°, V = 930.9(1) Å^3, Z = 2, D_c = 1.703 Mg M^{-3}, μ(Mo Kα) = 32.069 mm^{-1}, F(000) = 480, crystal size 0.50 × 0.40 × 0.30 mm^3; 4856 reflections measured, 3242 independent reflections (R_{int} = 0.0146), the final R was 0.0253 [$I > 2\sigma(I)$] and $wR(F^2)$ was 0.0637 (all data).

Crystal data for **13bH** (picrate): $C_{19}H_{16}N_4O_7Se$, M = 491.32, T = 130.0(2) K, λ = 1.5418 Å, monoclinic, space group $P2_1/n$, a = 11.6919(2) Å, b = 8.2865(2) Å, c = 20.4393(4) Å, β = 97.802(2)°, V = 1961.93(7) Å^3, Z = 4, D_c = 1.663 Mg M^{-3}, μ(Cu Kα) = 3.066 mm^{-1}, F(000) = 992, crystal size 0.6 × 0.4 × 0.2 mm^3; 8689 reflections measured, 3853 independent reflections (R_{int} = 0.0181), the final R was 0.0297 [$I > 2\sigma(I)$] and $wR(F^2)$ was 0.0825 (all data).

b. Synthesis:

General. All reactions were performed in oven-dried glassware under nitrogen atmosphere. Anhydrous ethanol was distilled from magnesium ethoxide under nitrogen atmosphere. Deuterated solvents were stored over 4 Å sieves before use. Products were purified via crystallization with *n*-pentane. Proton nuclear magnetic resonance spectra (^{1}H NMR, 400 and 500 MHz) and proton decoupled carbon nuclear magnetic resonance spectra (^{13}C NMR, 100 and 125 MHz) were obtained in deuterioacetonitrile or deuteriochloroform with residual acetonitrile or chloroform as internal standards. Selenium nuclear magnetic resonance (^{77}Se NMR, 95 MHz) was performed in deuterioacetonitrile or deuteriochloroform with an external standard consisting of diphenyl diselenide in deuteriochloroform (100 mg/1 mL), which was referenced at 464 ppm. Chemical shifts are reported in parts per million (ppm), followed by (in parentheses, where applicable) multiplicity, coupling constant(s) (J, Hz), integration, and assignments. High-resolution mass spectra (HRMS) were obtained by ionizing samples via electron spray ionization (ESI). Mass spectra are expressed as mass to charge ratio (m/z) values. Melting points were uncorrected. Assignment of the methylene carbons for the benzylselenylmethyl pyridine and pyridinium ions (**10b**, **11b**, **12b**, and **13b**) was achieved by using 2-dimensional NMR techniques. ^{1}H NMR assignment was supported by gCOSY experiments and ^{13}C NMR assignment by DEPT experiments, as well as gHSQC and gHMBC two-dimensional experiments.

(Phenylselenomethyl)pyridines 12a, and 13a: General Procedure. To a solution of diphenyl diselenide (1.00 mmol) in 20 mL of anhydrous ethanol was added sodium borohydride (in excess) portionwise until the solution turn colorless. Meanwhile, to a stirred suspension of the appropriate bromomethyl pyridine hydrobromide (2.00 mmol) in 25 mL of ethanol at 0 °C was added ice-cold 1 M NaOH solution (2.00 mmol, 2 mL) in 8 mL of ethanol. This cold solution was stirred for another 10 min then added dropwise at room temperature into the anion solution previously generated. The reaction mixture was left to stir overnight under nitrogen, then diluted with 25 mL of diethyl ether and washed with water (5 × 20 mL). A 1 M HCl solution was added to the organic phase and the product was extracted into the acidic aqueous phase (3 × 20 mL), which was then neutralized with 1 M NaOH solution. The pure product was extracted from the neutralized solution by using diethyl ether (3 × 20 mL), washed with water (3 × 20 mL) and then brine (3 × 20 mL), and dried over magnesium sulfate, then solvent was removed under reduced pressure to afford the pure product.

4-(Phenylselenomethyl)pyridine, 12a:. 0.22 g (89%); yellow oil; ^{1}H NMR (CD_3CN, 500 MHz) δ 8.40 (d, J = 4.4 Hz, 2H, Ar-*H*), 7.46 (m, 2H, Ar-*H*), 7.29 (m, 3H, Ar-*H*), 7.14 (d, J = 4.4 Hz, 2H, Ar-*H*), 4.10 (s, 2H, $-CH_2$); ^{13}C NMR ($CDCl_3$, 125 MHz) δ 150.7 (Ar-*C*), 149.3 (Ar-C), 138.4 (Ar-*C*), 134.4 (Ar-C), 130.2 (Ar-*C*), 128.6 (Ar-C), 124.8 (Ar-C), 30.6 ($^1J_{C-Se}$ = 61.9 Hz, $-CH_2$); ^{77}Se NMR (95 MHz, sample in CD_3CN, external standard: $(PhSe)_2$ in $CDCl_3$) δ 361.2; HRMS (ESI) calcd for $C_{12}H_{12}NSe^+$ $[M + H]^+$ 250.01295, found 250.01298; IR (thin film) $\tilde{\nu}$ 3062−2927 cm^{-1} (pyridine ring).

2-(Phenylselenomethyl)pyridine, 13a:. 0.21 g (86%); yellow oil; ^{1}H NMR (CD_3CN, 500 MHz) δ 8.44 (d, J = 4.9 Hz, 1H, Ar-*H*), 7.59 (td, J = 7.7, 1.9 Hz, 1H, Ar-*H*), 7.49 (m, 2H, Ar-*H*), 7.25 (m, 4H, Ar-*H*), 7.14 (m, 1H, Ar-*H*), 4.25 (s, 2H, $-CH_2$); ^{13}C NMR (CD_3CN, 125 MHz) δ 160.0 (Ar-*C*), 150.2 (Ar-C), 137.5 (Ar-*C*), 133.6 (Ar-C), 131.3 (Ar-C), 130.1 (Ar-C), 128.1 (Ar-C), 123.9 (Ar-C), 122.8 (Ar-C), 33.9 ($^1J_{C-Se}$ = 61.9 Hz, $-CH_2$); ^{77}Se NMR (95 MHz, sample in CD_3CN, external standard: $(PhSe)_2$ in $CDCl_3$) δ 337.2; HRMS (ESI) calcd for $C_{12}H_{12}NSe^+$ $[M + H]^+$ 250.01295, found 250.01291; IR (thin film) $\tilde{\nu}$ 3077−2938 cm^{-1} (pyridine ring).

***N*-Methyl 4-(phenylselenomethyl)pyridinium triflate, 10a:.** A solution of **12a** (50.0 mg, 0.20 mmol) in 0.5 mL of deuterioacetonitrile was treated with neat methyl triflate (36.4 mg, 0.22 mmol, 25.1 μL). After evaporation of the solvent **10a** as its triflate salt was obtained as a yellow oil: ^{1}H NMR (CD_3CN, 500 MHz) δ 8.40 (d, J = 6.6 Hz, 2H, Ar-*H*), 7.60 (d, J = 6.8 Hz, 2H, Ar-*H*), 7.48−7.25 (m, 5H, Ar-*H*), 4.25 (s, 2H, $-CH_2$), 4.20 (s, 3H, $-CH_3$); ^{13}C NMR (CD_3CN, 125 MHz) δ 161.2 (Ar-C), 150.0 (Ar-*C*), 145.6 (Ar-C), 135.6 (Ar-C), 130.6 (Ar-*C*), 129.6 (Ar-C), 128.2 (Ar-*C*), 48.6 ($-CH_3$), 30.2 ($^1J_{C-Se}$ = 65.5 Hz, $-CH_2$); ^{77}Se NMR (95 MHz, sample in CD_3CN, external standard: $(PhSe)_2$ in $CDCl_3$) δ 406.8; HRMS (ESI) calcd for $C_{13}H_{14}NSe^+$ $[M]^+$ 264.02860, found 264.02856; IR (thin film) $\tilde{\nu}$ 3062−2927 cm^{-1} (pyridine ring).

***N*-Methyl 2-(phenylselenomethyl)pyridinium triflate, 11a:.** A solution of **13a** (50.0 mg, 0.20 mmol) in 0.5 mL of deuterioacetonitrile was treated with neat methyl triflate (36.4 mg, 0.22 mmol, 25.1 μL). X-ray quality crystals of **11a** were obtained from slow evaporation of solvent: crystalline plates; mp 118.3−120.3 °C; ^{1}H NMR (CD_3CN, 500 MHz) δ 8.63 (d, J = 6.2 Hz, 1H, Ar-*H*), 8.09 (t, J = 7.9 Hz, 1H, Ar-*H*), 7.75 (t, J = 7.0 Hz, 1H, Ar-*H*), 7.45−7.29 (m, 5H, Ar-*H*), 7.24 (d, J = 7.5 Hz, 1H, Ar-*H*), 4.41 (s, 2H, $-CH_2$), 4.26 (s, 3H, $-CH_3$); ^{13}C NMR (CD_3CN, 125 MHz) δ 156.1 (Ar-*C*), 148.0 (Ar-C), 145.9 (Ar-C), 137.0 (Ar-C), 132.1 (Ar-C), 130.6 (Ar-C), 130.4 (Ar-C), 129.9 (Ar-C), 126.9 (Ar-C), 46.6 ($-CH_3$), 27.8 ($^1J_{C-Se}$ = 67.7 Hz, $-CH_2$); ^{77}Se NMR (95 MHz, sample in CD_3CN, external standard: $(PhSe)_2$ in $CDCl_3$) δ 364.9; HRMS (ESI) calcd for $C_{13}H_{14}NSe^+$ $[M]^+$ 264.02860, found 264.02856; IR (thin film) $\tilde{\nu}$ 3062−2927 cm^{-1} (pyridine ring).

Preparation of 4-(phenylselenomethyl)pyridinium picrate, 12aH:. To a solution of **12a** (50.0 mg, 0.20 mmol) in 2 mL of anhydrous ethanol was added picric acid (46.2 mg, 0.20 mmol) at room temperature. The reaction was left to stir overnight under nitrogen. Ethanol was removed under reduced pressure to afford the product in solid form. X-ray quality crystals of **12aH** were obtained from chloroform/diethyl ether diffusion as yellow needles: mp 155.3−157.3 °C; ^{1}H NMR ($CDCl_3$, 500 MHz) δ 8.58 (d, J = 7.1 Hz, 2H, Ar-*H*), 7.42 (m, 4H, Ar-*H*), 7.31 (m, 3H, Ar-*H*), 4.12 (s, 2H, $-CH_2$), 9.05 (s, 2H, Ar-*H*); ^{13}C NMR ($CDCl_3$, 125 MHz) δ 160.0 (Ar-*C*), 141.9 (Ar-C), 132.5 (Ar-C), 130.9 (Ar-C), 130.6 (Ar-C), 127.6 (Ar-C), 127.3 (Ar-C), 31.7 ($^1J_{C-Se}$ = 67.0 Hz, $-CH_2$), 161.6 (Ar-C), 140.8 (Ar-C), 136.6 (Ar-C), 127.5 (Ar-C); ^{77}Se NMR (95 MHz, sample in $CDCl_3$, external standard: $(PhSe)_2$ in $CDCl_3$) δ 419.2; HRMS (ESI) calcd for $C_{12}H_{12}NSe^+$ $[M]^+$ 250.01295, found 250.01298; IR (thin film) $\tilde{\nu}$ 3062−2927 cm^{-1} (pyridine ring).

(Benzylselenomethyl)pyridines: General Procedure. To a solution of dibenzyl diselenide (1.00 mmol) in 20 mL of anhydrous ethanol was added sodium borohydride (in excess) portionwise until the

solution turn colorless. Meanwhile, to a stirred suspension of the appropriate bromomethyl pyridine hydrobromide (2.00 mmol) in 25 mL of ethanol at 0 °C was added ice-cold 1 M NaOH solution (2.00 mmol, 2 mL) in 8 mL of ethanol. This cold solution was stirred for another 10 min then added dropwise at room temperature into the anion solution previously generated. The reaction mixture was left to stir overnight under nitrogen. Ethanol was removed under reduced pressure and the residue was taken up in diethyl ether (25 mL), 1 M HCl solution was added to the organic phase, and the product was extracted into the acidic aqueous phase (3 × 20 mL), which was then neutralized with 1 M NaOH solution. The pure product was extracted from the neutralized solution by using diethyl ether (3 × 20 mL), washed with water (3 × 20 mL) and then brine (3 × 20 mL), and dried over $MgSO_4$, and then solvent was removed under reduced pressure to afford the product. Solid product was crystallized in *n*-pentane.

2-(Benzylselenomethyl)pyridine, 13b:. 0.47 g (92%); crystalline plates; mp 28.5−29.8 °C; ^{1}H NMR ($CDCl_3$, 500 MHz) δ 8.53 (d, J = 5.0 Hz, 1H, Ar-*H*), 7.61 (ddd, J = 8.0, 8.0, 1.5 Hz, 1H, Ar-*H*), 7.33−7.19 (m, 5H, Ar-*H*), 7.14 (t, J = 6.0 Hz, 2H, Ar-*H*), 3.86 (s, 2H, $-CH_2$), 3.85 (s, 2H, $-CH_2$); ^{13}C NMR ($CDCl_3$, 100 MHz) δ 159.4 (Ar-*C*), 148.9 (Ar-*C*), 138.8 (Ar-*C*), 136.2 (Ar-*C*), 128.7 (Ar-*C*), 128.1 (Ar-*C*), 126.3 (Ar-*C*), 122.6 (Ar-*C*), 121.2 (Ar-*C*), 28.7 ($^1J_{C-Se}$ = 64.8 Hz, $-CH_2$), 27.3 ($-CH_2$); ^{77}Se NMR (95 MHz, sample in $CDCl_3$, external standard: $(PhSe)_2$ in $CDCl_3$) δ 331.3; HRMS (ESI) calcd for $C_{13}H_{14}NSe^+$ $[M + H]^+$ 264.02860, found 264.02862; IR (thin film) $\tilde{\nu}$ 3077−2938 cm^{-1} (pyridine ring).

4-(Benzylselenomethyl)pyridine, 12b:. 0.48 g (93%); crystalline plates; mp 33.3−34.9 °C; ^{1}H NMR (CD_3CN, 500 MHz) δ 8.47 (dd, J = 4.0, 1.8 Hz, 2H, Ar-*H*), 7.34−7.23 (m, 5H, Ar-*H*), 7.22 (dd, J = 4.5, 2.0 Hz, 2H, Ar-*H*), 3.81 (s, 2H, $-CH_2$), 3.73 (s, 2H, $-CH_2$); ^{13}C NMR (CD_3CN, 125 MHz) δ 150.8 (Ar-*C*), 150.1 (Ar-*C*), 140.4 (Ar-*C*), 129.9 (Ar-*C*), 129.6 (Ar-*C*), 127.8 (Ar-*C*), 124.9 (Ar-*C*), 28.4 ($-CH_2$), 26.6 ($^1J_{C-Se}$ = 65.5 Hz, $-CH_2$); ^{77}Se NMR (95 MHz, sample in CD_3CN, external standard: $(PhSe)_2$ in $CDCl_3$) δ 338.1; HRMS (ESI) calcd for $C_{13}H_{14}NSe^+$ $[M + H]^+$ 264.02860, found 264.02798; IR (thin film) $\tilde{\nu}$ 3062−2927 cm^{-1} (pyridine ring).

***N*-Methyl-2-(benzylselenomethyl)pyridinium triflate, 11b:.** A solution of **13b** (50.0 mg, 0.19 mmol) in 0.5 mL of deuterioacetonitrile was treated with neat methyl triflate (34.0 mg, 0.21 mmol, 24 μL). After removal of the solvent **11b** was obtained as a pale yellow oil; ^{1}H NMR (CD_3CN, 500 MHz) δ 8.57 (d, J = 5.5 Hz, 1H, Ar-*H*), 8.31 (td, J = 7.9, 1.5 Hz, 1H, Ar-*H*), 7.77 (t, J = 6.6 Hz, 1H, Ar-*H*), 7.46 (m, 1H, Ar-*H*), 7.34−7.24 (m, 5H, Ar-*H*), 4.17 (s, 3H, $-CH_3$), 4.13 (s, 2H, $-CH_2$), 3.99 (s, 2H, $-CH_2$); ^{13}C NMR (CD_3CN, 125 MHz) δ 156.8 (Ar-*C*), 148.1 (Ar-*C*), 146.6 (Ar-*C*), 139.0 (Ar-*C*), 131.7 (Ar-*C*), 130.1 (Ar-*C*), 129.8 (Ar-*C*), 128.3 (Ar-*C*), 126.9 (Ar-*C*), 46.4 ($-CH_3$), 29.5 ($^1J_{C-Se}$ = 61.7 Hz, $-CH_2$), 23.4 ($-CH_2$); ^{77}Se NMR (95 MHz, sample in CD_3CN, external standard: $(PhSe)_2$ in $CDCl_3$) δ 312.2; HRMS (ESI) calcd for $C_{14}H_{16}NSe^+$ $[M + H]^+$ 278.04425, found 278.04428; IR (thin film) $\tilde{\nu}$ 3072−2920 cm^{-1} (pyridine ring).

2-(Benzylselenomethyl)pyridinium picrate, 13bH:. To a solution of **13b** (50.0 mg, 0.19 mmol) in 2 mL of anhydrous ethanol was added picric acid (43.7 mg, 0.19 mmol) at room temperature. Reaction was left to stir overnight under nitrogen. Ethanol was removed under reduced pressure and the resulting solids were dissolved in a minimum amount of chloroform. X-ray quality crystals of **13b** were obtained from slow evaporation of solvent: yellow blocks; mp 122.1−123.0 °C; ^{1}H NMR ($CDCl_3$, 500 MHz) δ 8.66 (d, J = 5.5 Hz, 1H, Ar-*H*), 8.13 (td, J = 7.9, 1.5 Hz, 1H, Ar-*H*), 7.63 (t, J = 6.6 Hz, 1H, Ar-*H*), 7.48 (d, J = 8.1 Hz, 1H, Ar-*H*), 7.22−7.12 (m, 5H, Ar-*H*), 4.30 (s, 2H, $-CH_2$), 3.96 (s, 2H, $-CH_2$), 8.93 (s, 2H, Ar-*H*); ^{13}C NMR ($CDCl_3$, 125 MHz) δ 157.5 (Ar-*C*), 144.5 (Ar-*C*), 141.4 (Ar-*C*), 137.5 (Ar-*C*), 129.0 (Ar-*C*), 129.0 (Ar-*C*), 127.2 (Ar-*C*), 126.5 (Ar-*C*), 124.0 (Ar-*C*), 29.4 ($^1J_{C-Se}$ = 62.7 Hz, $-CH_2$), 22.8 ($-CH_2$), 161.3 (Ar-*C*), 141.5 (Ar-*C*), 129.3 (Ar-*C*), 128.6 (Ar-*C*); ^{77}Se NMR (95 MHz, sample in $CDCl_3$, external standard: $(PhSe)_2$ in $CDCl_3$) δ 375.6; HRMS (ESI) calcd for $C_{13}H_{14}NSe^+$ $[M + H]^+$ 264.02860, found 264.02862; IR (thin film) $\tilde{\nu}$ 3067−2910 cm^{-1} (pyridine ring).

***N*-Methyl-4-(benzylselenomethyl)pyridinium triflate, 10b:.** A solution of **12b** (50.0 mg, 0.19 mmol) in 0.5 mL of deuterioacetonitrile was treated with neat methyl triflate (34.0 mg, 0.21 mmol, 24 μL). X-ray quality crystals of **10b** as plates were obtained by slow evaporation of solvent: mp 79.2−82.2 °C; ^{1}H NMR (CD_3CN, 500 MHz) δ 8.39 (d, J = 6.5 Hz, 2H, Ar-*H*), 7.73 (d, J = 6.0 Hz, 2H, Ar-*H*), 7.32−7.26 (m, 5H, Ar-*H*), 4.21 (s, 3H, $-CH_3$), 3.93 (s, 2H, $-CH_2$), 3.90 (s, 2H, $-CH_2$); ^{13}C NMR (CD_3CN, 100 MHz) δ 162.2 (Ar-*C*), 145.6 (Ar-*C*), 139.6 (Ar-*C*), 130.1 (Ar-*C*), 129.7 (Ar-*C*), 128.6 (Ar-*C*), 128.1 (Ar-*C*), 48.6 ($-CH_3$), 28.9 ($-CH_2$), 26.1 ($^1J_{C-Se}$ = 67.0 Hz, -CH_2); ^{77}Se NMR (95 MHz, sample in CD_3CN, external standard: $(PhSe)_2$ in $CDCl_3$) δ 376.9; HRMS (ESI) calcd for $C_{14}H_{16}NSe^+$ $[M]^+$ 278.04425, found 278.04422; IR (thin film) $\tilde{\nu}$ 3027−2963 cm^{-1} (pyridine ring).

4-(Benzylselenomethyl)pyridinium trifluoroacetate, 12bH:. A solution of **12b** (50.0 mg, 0.19 mmol) in 0.5 mL of deuteriochloroform was treated with neat trifluoroacetic acid (26.1 mg, 0.23 mmol, 17.5 μL): ^{77}Se NMR (95 MHz, sample in $CDCl_3$, external standard: $(PhSe)_2$ in $CDCl_3$) δ 375.1.

(*tert*-Butylselenomethyl)pyridine: General Procedure. To a solution of bis(2-methyl-2-propyl) diselenide (di-*tert*-butyl diselenide) (1.29 mmol) in 20 mL of anhydrous ethanol was added sodium borohydride (in excess) portionwise until the solution turned colorless. Meanwhile, to a stirred suspension of the appropriate bromomethyl pyridine hydrobromide (2.58 mmol) in 25 mL of ethanol at 0 °C was added ice-cold 1 M NaOH solution (2.58 mmol, 2.6 mL) in 9 mL of ethanol. This cold solution was stirred for another 10 min then added dropwise at room temperature into the anion solution previously generated. The reaction mixture was left to stir overnight under nitrogen. Ethanol was removed under reduced pressure and the residue was taken up in diethyl ether (25 mL) [alternatively, the reaction mixture was diluted with 25 mL of diethyl ether then washed with water (5 × 20 mL) to remove ethanol]. A 1 M HCl solution was added to the organic phase and the product was extracted into the acidic aqueous phase (3 × 20 mL), which was then neutralized with 1 M NaOH solution. The pure product was extracted from the neutralized solution with diethyl ether (3 × 20 mL), washed with water (3 × 20 mL) and then brine (3 × 20 mL), and dried over magnesium sulfate, then the solvent was removed under reduced pressure to afford the product. Solid product was crystallized in *n*-pentane.

2-(*tert*-Butylselenomethyl)pyridine, 13c:. 0.48 g (81%); pale yellow oil; ^{1}H NMR (CD_3CN, 500 MHz) δ 8.44 (dd, J = 4.9, 0.7 Hz, 1H, Ar-*H*), 7.65 (td, J = 7.8, 1.9 Hz, 1H, Ar-*H*), 7.39 (d, J = 8.0 Hz, 1H, Ar-*H*), 7.15 (ddd, J = 7.4, 4.9, 0.9 Hz, 1H, Ar-*H*), 3.99 (s, 2H, $-CH_2$), 1.47 (s, 9H, $-C(CH_3)_3$); ^{13}C NMR (CD_3CN, 125 MHz) δ 161.3 (Ar-*C*), 150.0 (Ar-*C*), 137.5 (Ar-*C*), 124.2 (Ar-*C*), 122.4 (Ar-*C*), 40.6 ($-C(CH_3)_3$), 32.7 (3C, $-C(CH_3)_3$), 28.6 ($^1J_{C-Se}$ = 67.7 Hz, $-CH_2$); ^{77}Se NMR (95 MHz, sample in CD_3CN, external standard: $(PhSe)_2$ in $CDCl_3$) δ 448.1; HRMS (ESI) calcd for $C_{10}H_{16}NSe^+$ $[M + H]^+$ 230.04425, found 230.04426.

4-(*tert*-Butylselenomethyl)pyridine, 12c:. 0.46 g (78%); colorless plates; mp 31.9−33.5 °C; ^{1}H NMR (CD_3CN, 500 MHz) δ 8.45 (d, J = 4.4 Hz, 2H), 7.30 (d, J = 4.3 Hz, 2H), 3.85 (s, 2H), 1.48 (s, 9H); ^{13}C NMR (CD_3CN, 125 MHz) δ 150.8, 150.4, 125.1, 41.3, 32.7, 25.0 ($^1J_{C-Se}$ = 67.3 Hz, $-CH_2$); ^{77}Se NMR (95 MHz, sample in CD_3CN, external standard: $(PhSe)_2$ in $CDCl_3$) δ 458.6; HRMS (ESI) calcd for $C_{10}H_{16}NSe^+$ $[M + H]^+$ 230.04425, found 230.04430.

***N*-Methyl-2-(*tert*-butylselenomethyl)pyridinium tosylate, 11c:.** A solution of **13c** (60.8 mg, 0.27 mmol) in 0.5 mL of deuteroacetonitrile was treated with neat methyl tosylate (54.6 mg, 0.29 mmol, 44.2 μL). X-ray quality crystals of **11c** were obtained from slow

evaporation of solvent: colorless plates; mp 130.2−133.7 °C; ^{1}H NMR (CD_3CN, 500 MHz) δ 8.66 (s, br, 1H, Ar-*H*), 8.36 (t, J = 7.9 Hz, 1H, Ar-*H*), 8.00 (d, J = 7.8 Hz, 1H, Ar-*H*), 7.80 (t, J = 6.9 Hz, 1H, Ar-*H*), 4.30 (s, 3H, $-CH_3$), 4.22 (s, 2H, $-CH_2$), 1.55 (s, 9H, $-C(CH_3)_3$), 7.60 (d, J = 8.2 Hz, 2H, Ar-*H*), 7.15 (d, J = 8.1 Hz, 2H, Ar-*H*), 2.34 (s, 3H, $-CH_3$); ^{13}C NMR (CD_3CN, 125 MHz) δ 157.5 (Ar-*C*), 148.3 (Ar-*C*), 146.7 (Ar-*C*), 130.4 (Ar-*C*), 126.9 (Ar-*C*), 46.5 ($-CH_3$), 44.3 ($-C(CH_3)_3$), 32.4 ($-C(CH_3)_3$), 21.9 ($^1J_{C-Se}$ = 70.5 Hz, $-CH_2$), 146.6 (Ar-*C*), 139.7 (Ar-*C*), 129.4 (Ar-*C*), 126.7 (Ar-*C*), 21.4 ($-CH_3$); ^{77}Se NMR (95 MHz, sample in CD_3CN, external standard: $(PhSe)_2$ in $CDCl_3$) δ 443.3; HRMS (ESI) calcd for $C_{11}H_{18}NSe^+$ $[M]^+$ 244.05990, found 244.05992; IR (thin film) $\tilde{\nu}$ 3042−2856 cm^{-1} (pyridine ring).

2-(*tert*-Butylselenomethyl)pyridinium trifluoroacetate, 13cH:. A solution of **13c** (50.0 mg mg, 0.22 mmol) in 0.5 mL of chloroform was treated with neat trifluoroacetic acid (30.0 mg, 0.26 mmol, 20.1 μL): ^{77}Se NMR (95 MHz, sample in $CDCl_3$, external standard: $(PhSe)_2$ in $CDCl_3$) δ 491.5.

***N*-Methyl-4-(*tert*-butylselenomethyl)pyridinium tosylate, 11c:.** A solution of **13c** (45.0 mg, 0.20 mmol) in 0.5 mL of deuterioacetonitrile was treated with neat methyl tosylate (40.4 mg, 0.22 mmol, 32.7 μL). X-ray quality crystals of **11c** were obtained by slow evaporation of the solvent: colorless plates; mp 161.4−162.4 °C; ^{1}H NMR (CD_3CN, 500 MHz) δ 8.60 (d, J = 6.6 Hz, 2H, Ar-*H*), 7.87 (d, J = 6.6 Hz, 2H, Ar-*H*), 4.24 (s, 3H, $-CH_3$), 4.03 (s, 2H, $-CH_2$), 1.47 (s, 9H, $-C(CH_3)_3$); [tosylate]$^-$ 7.60 (d, J = 8.3 Hz, 2H, Ar-*H*), 7.15 (d, J = 8.2 Hz, 2H, Ar-*H*), 2.35 (s, 3H, $-CH_3$); ^{13}C NMR (CD_3CN, 125 MHz) δ 162.3 (Ar-*C*), 146.0 (Ar-*C*), 128.8 (Ar-*C*), 48.5 ($-CH_3$), 43.2 ($-C(CH_3)_3$, 32.6 ($-C(CH_3)_3$), 24.6 ($^1J_{C-Se}$ = 70.9 Hz, $-CH_2$), 146.2 (Ar-*C*), 139.9 (Ar-*C*), 129.5 (Ar-*C*), 126.7 (Ar-*C*), 21.4 ($-CH_3$); ^{77}Se NMR (external standard: $(PhSe)_2$ in $CDCl_3$, 95 MHz) δ 495.0; HRMS (ESI) calcd for $C_{11}H_{18}NSe^+$ $[M]^+$ 244.05990, found 244.05995; IR (thin film) $\tilde{\nu}$ 3047−2912 cm^{-1} (pyridine ring).

4-(*tert*-Butylselenomethyl)pyridinium trifluoroacetate, 12cH:. A solution of **12c** (50.0 mg mg, 0.22 mmol) in 0.5 mL of chloroform was treated with neat trifluoroacetic acid (30.0 mg, 0.26 mmol, 20.1 μL): ^{77}Se NMR (95 MHz, sample in $CDCl_3$, external standard: $(PhSe)_2$ in $CDCl_3$) δ 490.1

■ ASSOCIATED CONTENT

Supporting Information. Crystallographic information files for **10b**, **10c**, **11a**, **11c**, **12aH**, **13aH**, and **13bH**, a full listing of geometries and energies (Gaussian Archive entries) (S1), and NMR spectra for new compounds (S2). This material is available free of charge via the Internet at http://pubs.acs.org. The crystallographic coordinates have been deposited with the Cambridge Crystallographic Data Centre; deposition nos. 800803−800809. These data can be obtained free of charge from the Cambridge Crystallographic Data Centre, 12 Union Rd., Cambridge CB2 1EZ, UK or via www.ccdc.cam.ac.uk/conts/retrieving.html.

■ AUTHOR INFORMATION

Corresponding Author
*E-mail: whitejm@unimelb.edu.au.

■ ACKNOWLEDGMENT

We thank the Australian Research Council for financial support (DP0770565) and an award of an APA to B.H. We would also like to thank the Victorian Partnership for Advanced Computing and the Victorian Institute for Chemical Sciences High Performance Computing Facility for the computational time. A grateful thanks is extended to Dr. Colin Skene for assistance in obtaining the 2-D NMR data for **10b**, **11b**, **12b**, and **13b**.

■ REFERENCES

(1) White, J. M.; Lambert, J. B.; Spiniello, M.; Jones, S. A.; Gable, R. W. *Chem.—Eur. J.* **2002**, *8*, 2799.

(2) Capon, B.; McManus, S. P., *Neighbouring group Participation*; Plenum Press: New York, 1976; Vol. 1.

(3) (a) Traylor, T. G.; Berwin, H. J.; Jerkunica, M. L. H. *Pure Appl. Chem.* **1972**, 599. (b) Hanstein, W.; Berwin, H. J.; Traylor, T. G. *J. Am. Chem. Soc.* **1970**, *92*, 829. (c) Hanstein, W.; Berwin, H. J.; Traylor, T. G. *J. Am. Chem. Soc.* **1970**, *92*, 7476. (d) Traylor, T. G.; Hanstein, W.; Berwin, H. J.; Clinton, N. A.; Brown, R. S. *J. Am. Chem. Soc.* **1971**, *93*, 5715.

(4) (a) Lambert, J. B. *Tetrahedron* **1990**, *46*, 2677. (b) Lambert, J. B.; Zhou, Y.; Emblidge, R. W.; Salvador, L. A.; Liu, X. Y.; So, J. H.; Chelius, E. C. *Acc. Chem. Res.* **1999**, *32*, 183. (c) White, J. M., Clark, C. Stereoelectronic Effects of Group 4 Metal substituents, In *Topics in Stereochemistry* Denmark, S., Ed.; John Wiley and Sons: New York, 1999; Vol. 22, Chapter 3. (d) White, J. M. *Aust. J. Chem.* **1995**, *48*, 1227–1251.

(5) Beaver, M. G.; Billings, S. B.; Woerpel, K. A. *Eur. J. Org. Chem.* **2008**, 771. Beaver, M. G.; Billings, S. B.; Woerpel, K. A. *J. Am. Chem. Soc.* **2008**, *130*, 2082.

(6) (a) Briggs, A. J.; Glenn, R.; Jones, P. G.; Kirby, A. J.; Ramaswamy, P. *J. Am. Chem. Soc.* **1984**, *106*, 6200. (b) Amos, R. D.; Handy, N. C.; Jones, P. G.; Kirby, A. J.; Parker, J. K.; Percy, J. M.; Su, M. D. *J. Chem. Soc., Perkin Trans. 2* **1992**, *4*, 549.

(7) (a) Karnezis, A.; O'Hair, R. A. J.; White, J. M. *Organometallics* **2009**, *28*, 6480–6488. (b) Hassall, K.; Schiesser, C. H.; White, J. M. *Organometallics* **2007**, *26*, 3094–3099. (c) Hassall, K.; Lobachevsky, S.; Schiesser, C. H.; White, J. M. *Organometallics* **2007**, *26*, 1361–1364. (d) Hassall, K.; Lobachevsky, S.; White, J. M. *J. Org. Chem.* **2005**, *70*, 1993–1997. (e) Happer, A.; Ng Hui Mian, J.; Pool, B.; White, J. M. *J. Organomet. Chem.* **2002**, *659*, 10–14.

(8) Tomoda, S.; Shimoda, M.; Takeuchi, Y. *Chem. Lett.* **1989**, 1373.

(9) Wrackmeyer, B.; Hernandez, Z. G.; Herberhold, M. *Magn. Reson. Chem.* **2007**, *45*, 198.

(10) The Cambridge Structural Database: a quarter of a million crystal structures and rising: Allen, F. H. *Acta Crystallogr.* **2002**, *B58*, 380.

(11) (a) Kirby, A. J. *The Anomeric Effect and Related Stereoelectronic Effects at Oxygen*; Springer-Verlag: New York, 1983. (b) *The Anomeric Effect and Associated Stereoelectronic Effects*, ACS Symp. Ser. No. 539; Thatcher, G. R. J., Ed.; American Chemical Society: Washington, DC, 1993.

(12) McLeod, R. G.; Johnson, B. D.; Pinto, B. M. *Isr. J. Chem.* **2000**, *40*, 307.

(13) Szabo, K. J.; Frisell, H.; Engman, L.; Piatek, M.; Oleksyn, B.; Sliwinski, J. *J. Mol. Struct.* **1998**, *448*, 21.

(14) Becke, A. D. *Phys. Rev.* **1988**, *38*, 3098.

(15) Alabugin, I. V.; Manoharan, M.; Zeidan, T. A. *J. Am. Chem. Soc.* **2002**, *124*, 3175.

(16) Glendening, E. D.; Reed, A. E.; Carpenter, J. E.; Weinhold, F. *NBO*, Version 3.1, Theoretical Chemistry Institute, University of Wisconsin: Madison, 1990.

(17) Frisch, M. J.; Trucks, G. W.; Schlegel, H. B.; Scuseria, G. E.; Robb, M. A.; Cheeseman, J. R.; Montgomery, J. A., Jr.; Vreven, T.; Kudin, K. N.; Burant, J. C.; Millam, J. M.; Iyengar, S. S.; Tomasi, J.; Barone, V.; Mennucci, B.; Cossi, M.; Scalmani, G.; Rega, N.; Petersson, G. A.; Nakatsuji, H.; Hada, M.; Ehara, M.; Toyota, K.; Fukuda, R.; Hasegawa, J.; Ishida, M.; Nakajima, T.; Honda, Y.; Kitao, O.; Nakai, H.; Klene, M.; Li, X.; Knox, J. E.; Hratchian, H. P.; Cross, J. B.; Bakken, V.; Adamo, C.; Jaramillo, J.; Gomperts, R.; Stratmann, R. E.; Yazyev, O.; Austin, A. J.; Cammi, R.; Pomelli, C.; Ochterski, J. W.; Ayala, P. Y.; Morokuma, K.; Voth, G. A.; Salvador, P.; Dannenberg, J. J.; Zakrzewski, V. G.; Dapprich, S.; Daniels, A. D.; Strain, M. C.; Farkas, O.; Malick, D. K.; Rabuck, A. D.; Raghavachari, K.; Foresman, J. B.; Ortiz, J. V.; Cui,

Q.; Baboul, A. G.; Clifford, S.; Cioslowski, J.; Stefanov, B. B.; Liu, G.; Liashenko, A.; Piskorz, P.; Komaromi, I.; Martin, R. L.; Fox, D. J.; Keith, T.; M. A.; Al-Laham, Peng, C. Y.; Nanayakkara, A.; Challacombe, M.; Gill, P. M. W.; Johnson, B.; Chen, W.; Wong, M. W.; Gonzalez, C.; Pople, J. A. *Gaussian 03*, Revision C.02; Gaussian, Inc., Wallingford, CT, 2004.

(18) Bunting, J. W. *Biorg. Chem.* **1991**, *19*, 456.

(19) Bunting, J. W. *Tetrahedron* **1987**, *43*, 4277.

(20) Deno, N. C.; Jaruzelski, J. J.; Schriesheim, A. *J. Am. Chem. Soc.* **1955**, *77*, 3044.

(21) Okamoto, K.; Takeuchi, K.; Komatsu, K.; Kubota, Y.; Ohara, R.; Arima, M.; Takahashi, K.; Waki, Y.; Shiraj, S. *Tetrahedron* **1983**, *39*, 4011.

(22) Breslow, R.; Groves, J. T. *J. Am. Chem. Soc.* **1970**, *92*, 984.